Towards Reducing the Need for Annotations in Digital Dermatology with Self-supervised Learning

Fabian Gröger[1][a], Philippe Gottfrois[2], Ludovic Amruthalingam[2][b], Alvaro Gonzalez-Jimenez[2],
Simone Lionetti[1][c], Alexander A. Navarini[2,3][d] and Marc Pouly[1][e]

[1]*Lucerne University of Applied Sciences and Arts, Rotkreuz, Switzerland*
[2]*Department of Biomedical Engineering, University of Basel, Allschwil, Switzerland*
[3]*Department of Dermatology, University Hospital of Basel, Switzerland*

Keywords: Self-supervised Learning, Pre-training, Transfer Learning, Dermatology, Medical Imaging.

Abstract: Training supervised models requires large amounts of labelled data, whose creation is often expensive and time-consuming, especially in the medical domain. The standard practice to mitigate the lack of annotated clinical images is to use transfer learning and fine-tune pre-trained ImageNet weights on a downstream task. While this approach achieves satisfactory performance, it still requires a sufficiently large dataset to adjust the global features for a specific task. We report on an ongoing investigation to determine whether self-supervised learning methods applied to unlabelled domain-specific images can provide better representations for digital dermatology compared to ImageNet. We consider ColorMe, SimCLR, BYOL, DINO, and iBOT, and present preliminary results on the evaluation of pre-trained initialization for three different medical tasks with mixed imaging modalities. Our intermediate findings indicate a benefit in using features learned by iBOT on dermatology datasets compared to conventional transfer learning from ImageNet classification.

1 INTRODUCTION

Current artificial intelligence applications to medical imaging often rely on Convolution Neural Networks (CNNs) trained in a supervised way. These models have shown remarkable performance across many tasks due to their ability to deal with raw image data (Brinker et al., 2019). CNNs typically require vast amounts of annotated data to achieve high levels of performance and robustness. However, medical images can be hard to obtain: The acquisition process needs to consider strict regulations, collection biases should be appropriately mitigated (Groh et al., 2021), and examples of rare conditions are challenging to find.

Dermatology is a field of medicine where image analysis can have a significant impact since many pathologies are visible with a naked eye and can easily be photographed. Two main types of images are usually considered: dermoscopy pictures taken with a dedicated device called "dermatoscope", which is almost in direct contact with the skin and offers magnification, and ordinary clinical images, which are instead collected with cameras that are not specifically designed for dermatology.

Although a diagnosis is usually reported in patient files, one typically needs to recruit and train several dermatologists to do a tedious labeling job if more detailed information is required. Moreover, for several medical conditions, it is hard to get experts to agree on a common answer (Jacob et al., 2021). This explains why the most popular general-purpose image dataset, ImageNet (Deng et al., 2009), has 200 times more pictures than the biggest public dermoscopy dataset and 2000 times more than the largest public clinical image collection (ISIC, 2016).

Transfer learning can leverage knowledge from a source task with plenty of data to perform a target task where data is limited. The most common approach to transfer learning is pre-training large models such as residual neural network (ResNet) on huge labeled image datasets. Models pre-trained on ImageNet are also widely used in the medical domain,

which is controversial since features extracted from natural images, may not be ideal representations in some medical contexts (Matsoukas et al., 2022).

Self-supervised learning (SSL) is a hybrid approach that strives to combine supervised and unsupervised learning and is also often used through pre-training followed by adaptation (Shurrab and Duwairi, 2021). It aims at learning semantically useful features by creating a supervised objective from a pool of unlabelled data without the need for human annotation. This objective is often called the *pretext task*. Learnt features can then be used in *downstream tasks* where annotated data is scarce. In recent years, SSL became popular also in the medical domain as large volumes of unlabelled data are easier to obtain than their annotated counterparts. Several works have demonstrated the effectiveness of this approach for detection and classification (Li et al., 2021), for detection and localization (Sowrirajan et al., 2021), and for segmentation (Xie et al., 2020).

In this paper, we report intermediate results from an ongoing investigation on using SSL to mitigate the need for annotated samples in dermatology. We train several prominent SSL algorithms on a mixed dataset of 250'000 skin images, both from dermoscopy and clinical pictures. We then research the impact of using these representations as a starting point for different medical imaging tasks in dermatology.

2 SELF-SUPERVISED LEARNING TECHNIQUES

In this section, we briefly review the different SSL techniques considered in this work.

2.1 ColorMe

ColorMe (Li et al., 2020) was specifically designed for applications in the medical domain and embeds inductive bias in its two pretext tasks. It uses an encoder to map the green channel of an image to a vector space. This is followed both by a decoder, which learns to reconstruct the pixel values of the red and blue channels and by a fully-connected layer, which learns to predict the overall color distribution of the red and blue channels.

2.2 SimCLR

A simple framework for contrastive learning of visual representations (SimCLR) (Chen et al., 2020) proposes to obtain different views of the same image with heavy data augmentation, called positive samples, and

minimize the distance between their representations. At the same time, the distance between views of different images in the same batch, the negative samples, is maximized. The encoder is typically a ResNet architecture followed by a projection head to be discarded after training.

2.3 BYOL

Bootstrap your own latent (BYOL) (Grill et al., 2020) compares embeddings of image views obtained from two networks, removing the need for negative samples. The first network is termed *online* and consists of an encoder, a projection head, and a prediction head. The second network is known as *target*, has the same architecture as the online network except for the prediction head, and its weights are an exponential moving average of the online network weights. The training objective is to match the online network's output with the target network's output using mean squared error.

2.4 DINO

Self-distillation with no labels (DINO) (Caron et al., 2021) uses a similar principle to BYOL, but it passes transformations of an image into two separate encoders, respectively the student and the teacher networks. Unlike previous SSL approaches the encoder is a vision transformer (ViT) (Dosovitskiy et al., 2020). The loss compares the probability outputs of both networks using cross-entropy. Only the weights of the student are updated via backpropagation, while the parameters of the teacher are an exponential moving average of the student.

2.5 iBOT

Image BERT pre-training with online tokenizer (iBOT) (Zhou et al., 2022) exploits inherent properties of ViTs to learn representations capturing local and global information. Similarly to DINO, iBOT uses a student network that is trained and a teacher network which is an exponential moving average. Its loss function is the sum of two cross-entropies. The first one compares the output of the two networks when they are given different views of the same image. And the second one, when the two networks are both passed the same view, but some patches are masked for the student, matches the outputs corresponding to those patches.

Table 1: Hyperparameters of the different self-supervised learning techniques.

Algorithm	Backbone	# Params	Optimizer	Batch size	Lr.	Scheduler
ColorMe	ResNet50	23 Mio.	SGD	50	1×10^{-3}	-
SimCLR	ResNet50	23 Mio.	Adam	160	3×10^{-5}	cosine
BYOL	ResNet50	23 Mio.	Adam	150	3×10^{-3}	cosine
DINO	ViT-tiny	5.4 Mio.	AdamW	56	5×10^{-4}	cosine
iBOT	ViT-tiny	5.4 Mio.	AdamW	56	5×10^{-4}	cosine

3 EXPERIMENTAL SETUP

3.1 Pre-training Data

The training data includes both dermoscopy and clinical images, with the hypothesis that there are common patterns in skin pictures taken at different magnifications. In total, we use 242'039 images from both public and private datasets as listed below.

- derm7pt (Kawahara et al., 2019), featuring 2'020 dermoscopy and clinical images of various skin pigmentation lesions.

- ISIC (ISIC, 2016), which consists of 107'208 dermoscopy images with a wide spectrum of pigmented skin lesions mostly on low-pigmentation skin. We exclude pictures overlapping with HAM10000 (Tschandl et al., 2018) as these are used in a downstream task.

- MED-NODE (Giotis et al.,), which includes 170 clinical images of pigmented skin lesions.

- SD-260 (Sun et al., 2016), containing 12'583 clinical images of 260 different skin conditions.

- Ph2 (Mendonça et al., 2013), containing 200 dermoscopy images of pigmented skin lesions.

- A private dataset of 119'858 clinical images, reflecting the data distribution encountered in a Swiss hospital. Pictures were taken using diverse reflex cameras by a trained photographer, were anonymized, and used with approval (EKNZ-2018-01074) from an ethical committee according to Swiss regulations.

3.2 Downstream Tasks

To evaluate the performance of the pre-training methods, we use three different downstream tasks, which were not present in the pre-training data.

- Fitzpatrick17k (Groh et al., 2021) is a public benchmark dataset containing 16'577 clinical images with skin condition annotations and skin type labels based on the Fitzpatrick scoring system.

The dataset contains labels with different granularity. This study used the coarsest level, which splits skin conditions into three main categories.

- PAD-UFES-20 (Pacheco et al., 2020) is a public benchmark dataset composed of clinical images collected from smartphone devices and patient metadata. The dataset consists of 1'373 patients, 1'641 skin lesions, and 2'298 images for six different diagnoses: three skin diseases and three skin cancers.

- HAM10000 (Tschandl et al., 2018) is a public benchmark dataset consisting of 10'015 dermoscopic images gathered from different cohorts. The collected cases include a representative sample of seven diagnostic categories of pigmented lesions.

All non-test data for downstream tasks were randomly split into training and validation sets with size 85% and 15% respectively. Each downstream task was evaluated using the test set defined by the dataset authors.

3.3 Architectures

The SSL algorithms considered can be split into two groups based on the backbone architecture they work with, which can be a CNN or a ViT. To ensure a fair comparison, at least within the same group, we used the very same model when possible. To further promote the correspondence between the two groups, we selected architectures that perform similarly on ImageNet. For the CNN-based models we chose ResNet-50, and for the ViT-based ones a tiny vision transformer (Dosovitskiy et al., 2020) with patch size of 16×16. The number of trainable parameters is therefore roughly 23 Mio. for ResNet-50 and 5.4 Mio. for ViT-tiny.

3.4 Hyperparameters

Table 1 gives some details about the hyperparameters for pre-training. All images are resized to 224×224 pixels and normalized. Further, the models are trained

Table 2: Macro-averaged F1 scores of various models and a baseline on the hold-out test set of the three open-source dermatology downstream tasks. After adding a linear layer, both freezing and fine-tuning the backbone are considered.

Evaluation	Pre-training	Fitzpatrick17k	PAD-UFES-20	HAM10000
Linear Eval.	Stratified sampling	33.4 %	18.0 %	14.0 %
	ImageNet	51.0 %	49.7 %	54.1 %
	ColorMe	44.8 %	42.2 %	47.0 %
	SimCLR	37.0 %	32.7 %	28.2 %
	BYOL	48.1 %	34.4 %	44.4 %
	DINO	46.7 %	44.2 %	57.2 %
	iBOT	53.0 %	58.2 %	72.0 %
Fine-tuned	ImageNet	72.1 %	61.5 %	79.0 %
	ColorMe	71.0 %	61.7 %	73.1 %
	iBOT	73.9 %	62.3 %	82.0 %

until the validation loss does not improve consecutively over five epochs. A full scan of hyperparameter space is not performed as this exceeds the scope of this paper and our available computational resources. However, we ensure that all models converge to a suitable solution by manually choosing an appropriate optimizer and tuning the learning rate. We use the same data augmentation policies described in the original paper introducing each pretext task.

3.5 Evaluation

To compare the representations learned by different pre-training strategies, we test them in two ways: using linear evaluation on frozen embeddings and fine-tuning the whole model. Both experiments are performed on all downstream tasks. For models using a ResNet backbone, we add the linear layer after the last average pooling layer. For ViT-based models, we follow the (Caron et al., 2021) and add a linear layer after the concatenation of the class token to the last four blocks in the model. In the fine-tuning experiment, the backbone and the linear classification head are trained together.

Finally, to better understand the utility of self-supervised pre-training in different low-data regimes, we also train a simple k-nearest neighbor (kNN) classifier that acts as a few-shot learner for the downstream tasks. This classifier learns from a random subset of the downstream task's labeled data and is evaluated on the same hold-out test set as the linear evaluation and the fine-tuning.

4 RESULTS

Scores that probe the ability of self-supervised pre-trained features to generalize to the three downstream tasks are reported in table 2. The upper half shows the performance of frozen pre-trained embeddings upon linear evaluation. All models show better results compared to the random stratified sampling baseline, which randomly samples the prediction independently of the input data with empirical class probabilities determined from the training set. However, we also observe that the results of ColorMe, SimCLR and BYOL are worse than the performance achieved by using ImageNet features. This indicates that models with a CNN backbone do not profit from domain-specific pre-training in our setting and are better off using general features such as the ones from ImageNet. A possible explanation for this is that such models have a strong inductive bias which benefits more from initialization using general pre-trained weights (Matsoukas et al., 2022). Features from a ViT backbone yield less uniform patterns in comparison with ImageNet. DINO is only able to outperform the general features in one of three tasks and only by 3%. On the other hand, the results clearly show that iBOT performs well across all tasks and yields an improvement over ImageNet initialization by 2%, 9.5%, and 17.9%, respectively.

The lower half of table 2 summarizes the performance upon fine-tuning the pre-trained features. Here we only report results for the reference ImageNet model and the two models which obtained the highest average scores in the CNN and ViT classes of SSL approaches, i.e. ColorMe and iBOT. Similar to the results from the linear evaluation, we observe that using iBOT as initialization yields the best performance for all downstream tasks. Furthermore, we notice that the gap between ColorMe and iBOT is smaller than using linear evaluation, indicating that with enough training data and trainable parameters, similar features can be learned. Comparing the performance in the linear and fine-tuned evaluation, we can also see that the improvement for iBOT on PAD-UFES-20 and HAM10000 is noticeably smaller with
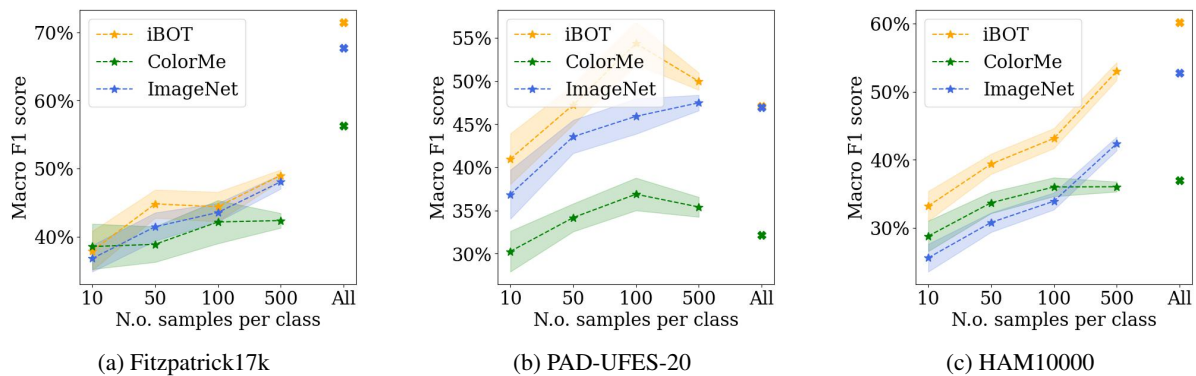
Figure 1: Results of a kNN classifier on pre-trained representations when varying the number of samples per class for all three downstream tasks.

respect to other methods. This suggests that the inherent structure of the dataset labels was already learned in the pre-training phase, and only minor adaptions to the existing features could be done.

Finally, figure 1 shows the results of adding a kNN classifier to the pre-trained ColorMe, iBOT and ImageNet features upon changing the training dataset size. The results achieved by iBOT outperform, on average, the ones from ImageNet over all three downstream tasks, indicating that its features are very competitive also in low data regimes.

5 CONCLUSION

In this paper, we set out to investigate whether features from domain-specific self-supervised pre-training yield a benefit over general-purpose ones such as ImageNet weights, which are currently the *de facto* standard in the medical domain. The results achieved so far indicate that there might be an advantage in SSL initialization, especially when using iBOT. However, we currently cannot conclude whether this benefit can be traced back to the pre-training strategy or the difference in model architecture. An indication in favor of the former is that DINO, which is also based on ViTs, did not outperform ImageNet initialization. In the future, we plan ablation experiments to determine if the performance gain is really due to the pre-training task or influenced by the different architecture.

REFERENCES

Brinker, T. J., Hekler, A., Enk, A. H., Berking, C., Haferkamp, S., Hauschild, A., Weichenthal, M., Klode, J., Schadendorf, D., Holland-Letz, T., von Kalle, C., Fröhling, S., Schilling, B., and Utikal, J. S. (2019).

Deep neural networks are superior to dermatologists in melanoma image classification. *European Journal of Cancer*, 119:11–17.

Caron, M., Touvron, H., Misra, I., Jégou, H., Mairal, J., Bojanowski, P., and Joulin, A. (2021). Emerging Properties in Self-Supervised Vision Transformers. pages 9650–9660.

Chen, T., Kornblith, S., Norouzi, M., and Hinton, G. (2020). A Simple Framework for Contrastive Learning of Visual Representations. In *Proceedings of the 37th International Conference on Machine Learning*, pages 1597–1607. PMLR.

Deng, J., Dong, W., Socher, R., Li, L.-J., Li, K., and Fei-Fei, L. (2009). Imagenet: A large-scale hierarchical image database. In *2009 IEEE Conference on Computer Vision and Pattern Recognition*, pages 248–255.

Dosovitskiy, A., Beyer, L., Kolesnikov, A., Weissenborn, D., Zhai, X., Unterthiner, T., Dehghani, M., Minderer, M., Heigold, G., Gelly, S., Uszkoreit, J., and Houlsby, N. (2020). An Image is Worth 16x16 Words: Transformers for Image Recognition at Scale.

Giotis, I., Molders, N., Land, S., Biehl, M., Jonkman, M., and Petkov, N. Med-node: A computer-assisted melanoma diagnosis system using non-dermoscopic images". *Expert Systems with Applications*, 42:6578–6585.

Grill, J.-B., Strub, F., Altché, F., Tallec, C., Richemond, P., Buchatskaya, E., Doersch, C., Avila Pires, B., Guo, Z., Gheshlaghi Azar, M., Piot, B., kavukcuoglu, k., Munos, R., and Valko, M. (2020). Bootstrap Your Own Latent - A New Approach to Self-Supervised Learning. In *Advances in Neural Information Processing Systems*, volume 33, pages 21271–21284. Curran Associates, Inc.

Groh, M., Harris, C., Soenksen, L., Lau, F., Han, R., Kim, A., Koochek, A., and Badri, O. (2021). Evaluating Deep Neural Networks Trained on Clinical Images in Dermatology with the Fitzpatrick 17k Dataset. pages 1820–1828. IEEE Computer Society.

ISIC (2016). ISIC Archive. https://www.isic-archive.com/. Accessed: 2022-05-20.

Jacob, J., Ciccarelli, O., Barkhof, F., and Alexander, D. C. (2021). Disentangling human error from the ground truth in segmentation of medical images. ACL.

Kawahara, J., Daneshvar, S., Argenziano, G., and Hamarneh, G. (2019). Seven-point checklist and skin lesion classification using multitask multimodal neural nets. *IEEE Journal of Biomedical and Health Informatics*, 23(2):538–546.

Li, X., Hu, X., Qi, X., Yu, L., Zhao, W., Heng, P.-A., and Xing, L. (2021). Rotation-Oriented Collaborative Self-Supervised Learning for Retinal Disease Diagnosis. *IEEE Transactions on Medical Imaging*, 40(9):2284–2294.

Li, Y., Chen, J., and Zheng, Y. (2020). A Multi-Task Self-Supervised Learning Framework for Scopy Images. In *2020 IEEE 17th International Symposium on Biomedical Imaging (ISBI)*, pages 2005–2009. ISSN: 1945-8452.

Matsoukas, C., Haslum, J. F., Sorkhei, M., Söderberg, M., and Smith, K. (2022). What Makes Transfer Learning Work For Medical Images: Feature Reuse & Other Factors. Technical Report arXiv:2203.01825, arXiv.

Mendonça, T., Ferreira, P. M., Marques, J. S., Marcal, A. R. S., and Rozeira, J. (2013). PH2 - A dermoscopic image database for research and benchmarking. In *2013 35th Annual International Conference of the IEEE Engineering in Medicine and Biology Society*.

Pacheco, A. G. C., Lima, G. R., Salomão, A. S., Krohling, B., Biral, I. P., de Angelo, G. G., Alves Jr, F. C. R., Esgario, J. G. M., Simora, A. C., Castro, P. B. C., Rodrigues, F. B., Frasson, P. H. L., Krohling, R. A., Knidel, H., Santos, M. C. S., do Espírito Santo, R. B., Macedo, T. L. S. G., Canuto, T. R. P., and de Barros, L. F. S. (2020). PAD-UFES-20: A skin lesion dataset composed of patient data and clinical images collected from smartphones. *Data in Brief*, 32:106221.

Shurrab, S. and Duwairi, R. (2021). Self-supervised learning methods and applications in medical imaging analysis: A survey. *arXiv:2109.08685 [cs, eess]*. arXiv: 2109.08685.

Sowrirajan, H., Yang, J., Ng, A. Y., and Rajpurkar, P. (2021). MoCo-CXR: MoCo Pretraining Improves Representation and Transferability of Chest X-ray Models. *arXiv:2010.05352 [cs]*.

Sun, X., Yang, J., Sun, M., and Wang, K. (2016). A benchmark for automatic visual classification of clinical skin disease images. In Leibe, B., Matas, J., Sebe, N., and Welling, M., editors, *Computer Vision – ECCV 2016*, pages 206–222, Cham. Springer International Publishing.

Tschandl, P., Rosendahl, C., and Kittler, H. (2018). The HAM10000 dataset, a large collection of multi-source dermatoscopic images of common pigmented skin lesions. *Scientific Data*, 5(1):180161.

Xie, Y., Zhang, J., Liao, Z., Xia, Y., and Shen, C. (2020). PGL: Prior-Guided Local Self-supervised Learning for 3D Medical Image Segmentation. *arXiv:2011.12640 [cs]*.

Zhou, J., Wei, C., Wang, H., Shen, W., Xie, C., Yuille, A., and Kong, T. (2022). ibot: Image bert pre-training with online tokenizer. *International Conference on Learning Representations (ICLR)*.